

Manipulation of Liquid Metals on a Graphite Surface

Liang Hu, Lei Wang, Yujie Ding, Shihui Zhan, and Jing Liu*

Liquid metals, such as eutectic gallium–indium (GaIn) and gallium–indium–tin (GaInSn) are quickly emerging as very important functional liquid-state metal materials with many unique properties, and have attracted wide attention from both academia and industry. However, it is still a big challenge to flexibly and stably control the shape of a liquid metal due to its extremely high surface tension. Here, a fundamental scientific finding is reported that a bouncing bright liquid-metal droplet in an alkaline electrolyte can be transformed to a flat and dull puddle when placed on a graphite surface. Through the intrinsic interactions between the liquid metal and the graphite, the liquid-metal puddle on the graphite can be manipulated as desired into various stable shapes with sharp angles in a semi-open space via a simple and highly feasible method. Moreover, it is also found that an electric field can be flexibly applied to control the transformation, locomotion, and even anti-gravity behavior of a liquid-metal puddle on graphite. Such phenomena are fundamentally different to those observed previously when placing liquid metals on a glass substrate. With basic science value and practical significance, the present finding suggests a pivotal strategy for liquid-metal patterning, as well as development of future soft mobile machines that have a 3D locomotion capability. It also adds new knowledge for understanding of liquid-metal science.

Nontoxic liquid metals (LMs), such as eutectic GaIn or GaInSn, are quickly emerging as innovative liquid-state metal materials at room temperature. With intriguing and valuable behaviors, such multifunctional materials are attracting increasing attention from both industry and academia. Their research categories have spanned from flexible and stretchable electronics^[1] and microfluidics^[2] to soft devices^[3,4] and chip cooling.^[5] Although LMs have already been investigated in some primary fields, further development has still not been as successful as anticipated, due to many unknown intrinsic properties of the liquid metals. Among those, the high surface tension of a liquid metal, which is ten times that of water,^[6] has been a big challenge for flexibly manipulating the liquid-metal structure. With a large surface tension, a liquid metal usually forms a droplet when interfaced with air or a liquid, which

makes it difficult for it to be shaped into desired structures for specific applications. To overcome this difficulty, tremendous efforts have been made recently, such that LMs were encapsulated into various molds via injection,^[7] gold-assisted deposition,^[8] localized stiff cell filling^[9] or dual-trans printing.^[10] However, the shaping mainly depends on enclosed molds and the surface tension of the LM remains high in those studies. The surface tension of LMs has also been reported to be altered electrochemically.^[3,11–13] However, the surface tension across the whole LM, as reported in those studies, was not so uniform and stable, since the electrochemical reactions over the LM surface are hard to control, which makes it difficult for them to form stable LM shapes. So far, the strategy to control the surface tension of an LM remains to be explored, since it has vital effects on shaping LMs for various practical controls as desired.

Apart from LM shaping, the high surface tension also evidently influences the locomotion of LM droplets in water. For example, the LM would move in a flow channel as a round spherical droplet due to the high surface tension. If the surface tension becomes much lower, the LM is more likely to be deformed under an external force, which in turn would influence the locomotion. However, the locomotion of an LM with much lower surface tension has rarely been reported up to now. As an unusual liquid-state metal material, LMs have already presented many promising properties for soft robot design and manufacture, including electrically^[13] or electrochemically^[3,4,12] drivable behaviors. Moreover, research on soft robots has kept gaining much attention in mobile machine design.^[14] The key challenge for soft machine manufacture lies in the development of controllable soft bodies using materials that can integrate sensors, actuators, and computation elements together to enable the body to deliver the desired behavior. The material with better stretchability and adaptability remains to be explored.

In this study, an intriguing and distinct phenomenon is discovered, such that when a spherical LM droplet is placed on a graphite substrate immersed in an electrolyte, it would easily become a dull, flat puddle. The mechanism underlying this straightforward transformation is due to the formation of an oxide layer on the droplet induced by the potential elevation upon contact with graphite. With significantly reduced surface tension, the shaping of the LM in the semi-open space in an electrolyte can now be achieved via a much easier operational way. Moreover, with unusual properties induced by the interaction with graphite, the dedicated locomotion of an LM on a graphite plane and slope when subjected to an electric field were also determined. The series of fundamental findings are expected to be important for the development of powerful ways of manipulating liquid metals in a liquid environment, and thus for soft machines in the near future.

It is known that LM EGaIn or GaInSn form bouncing spheres in an electrolyte due to its high surface tension at

Dr. L. Hu, Dr. L. Wang, Y. Ding, S. Zhan, Prof. J. Liu
Beijing Key Lab of CryoBiomedical Engineering
and Key Lab of Cryogenics
Technical Institute of Physics and Chemistry
Chinese Academy of Sciences
Beijing 100190, China
E-mail: liu@mail.ipc.ac.cn

Prof. J. Liu
Department of Biomedical Engineering
School of Medicine
Tsinghua University
Beijing 100084, China

DOI: 10.1002/adma.201601639



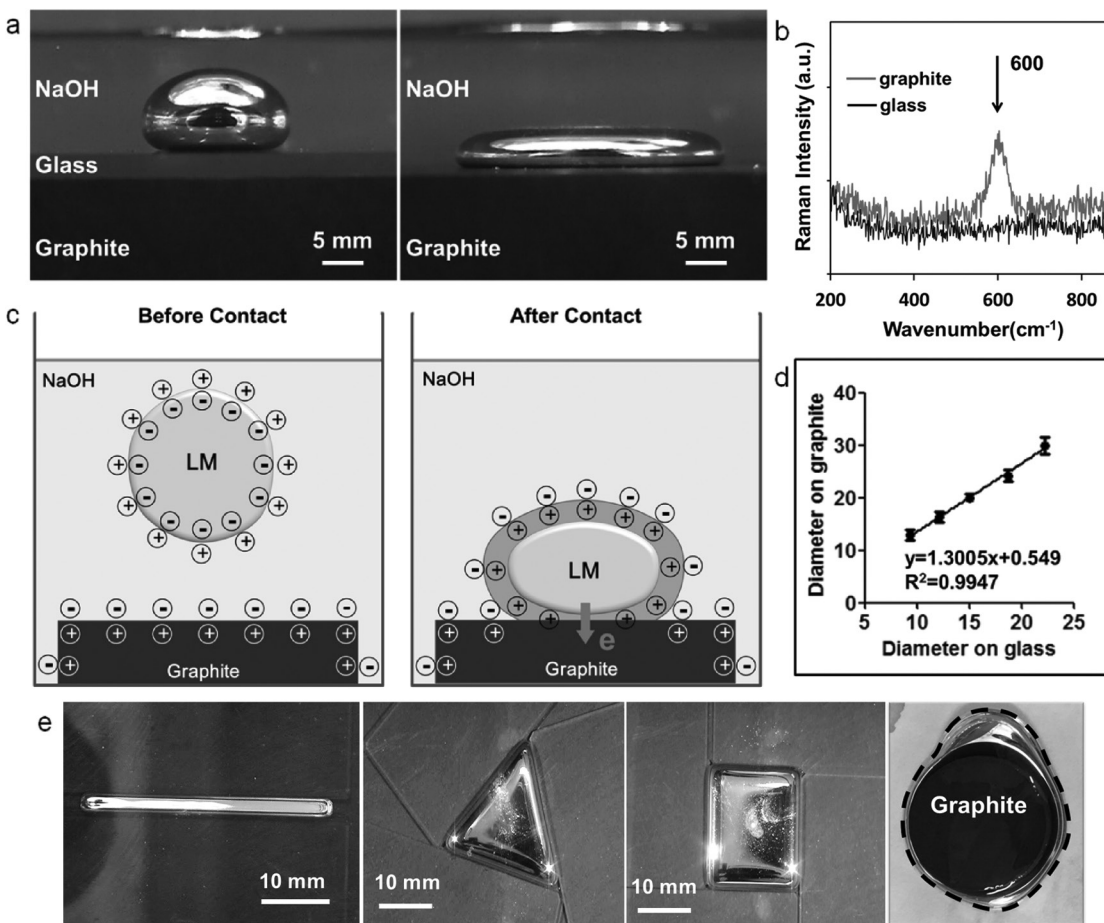


Figure 1. The transformation of the LM droplet on graphite in an electrolyte. a) Static images of an LM droplet on glass (left) and on a graphite substrate (right) in NaOH. The LM presented a quasi-sphere on the glass substrate and became flat on the graphite. b) Raman spectra of the LM droplet on graphite (gray) and on glass (black) in the 200–900 cm^{-1} region. c) Schematic figure of an LM interacting with a graphite substrate. The LM was electrochemically oxidized as the potential drop across the LM–NaOH was elevated due to contact with the graphite. d) Quantification of the diameter changes of the LM on glass and on graphite. e) Four typical basic shapes of LMs manipulated by glass slides including line, triangle, rectangle, and ring (the dashed line in the image on the far right indicates the LM).

room temperature. It has also been reported that liquid-metal droplets can transform from spheres into films under application of an external electric field.^[13,15] This transformation is due to the surface-tension changes induced by the electric field, which are quick and reversible by the removal of the electric field. In the present study, an LM droplet can quickly transform into a flat, dull puddle when placed on a graphite substrate immersed in an alkaline electrolyte (0.5×10^{-3} M NaOH solution in this work) (Movie S1, Supporting Information). The static images of the LM droplets on glass or graphite substrates immersed in 0.5×10^{-3} M NaOH are shown in Figure 1a. Besides, an oxidized membrane was observed on the LM puddle, which was composed of $\beta\text{-Ga}_2\text{O}_3$, confirmed by Raman measurements (as the appearance of a 600 cm^{-1} peak shift, Figure 1b).^[16] The surface tension was reduced by the interaction with the graphite substrate without an external electrical energy supply. When separated from the graphite, the dull, flat puddle quickly becomes a bouncing spherical droplet again in NaOH solution within 0.5 s (Movie S2, Supporting Information).

The mechanism underlying this flattening deformation is mainly related to the change of surface tension induced by the formation of an oxide layer on the LM puddle. The quick formation of this oxide layer should be caused by an electrochemical reaction induced by the graphite. Thus, it was predicted that the potential drop across the LM–NaOH interface was increased upon the LM–graphite contact. To testify this prediction, the zeta potential of graphite nanoparticles in NaOH was measured to evaluate the surface potential of graphite. At pH 11.6, the zeta potential of graphite was -31.6 mV , which indicates that there was a positive potential drop across the graphite–NaOH interface. Upon contact with the graphite, the negative potential drop across the LM–NaOH interface could be significantly elevated in order to reach to an equal potential to the graphite (Figure 1c). Thus, our prediction that the LM was electrochemically oxidized with abundant electrons quickly outflowing from LM to graphite was proven, which reduced the surface tension as a result. The zeta potentials of other conductive substrate materials including Cu and steel were also measured (Table S1, Supporting Information). A similar flattening behavior of LM

droplets was also observed on a copper substrate, which, however, should be mainly caused by the diffusion of gallium with copper. The zeta-potential results also confirmed that this flattening is not related to interface potential changes, as the potential drop across the copper–NaOH was negative, similar to that of LM and NaOH, while on a steel substrate, such an obvious flattening of the LM was not observed, which is also consistent with the the zeta-potential result. These results further confirm our prediction that the potential drop across the contact substrate and electrolyte interface plays the key role in such a flattening behavior of the LM.

As the surface tension of the LM droplets was reduced by the LM–graphite interaction, the bouncing LM droplets quickly became a flattened dull puddle. To quantify the transformation, the diameters of the same LM droplets on common glass and on graphite surfaces were measured. As shown in Figure 1d, the diameter of LM droplets measured on a graphite surface increased with the size of the original droplet in a linear manner, and the slope k is around 1.30. Moreover, several basic geometrical LM shapes including lines, triangles, rectangles, and rings were formed with simple slide molds, as shown in Figure 1e. Compared with an LM on a glass surface, it was easy to reshape the LM droplets into these other shapes, which have sharp angles, using the slides, while the LM droplet on glass retained a quasi-circle shape; this implies the effect of the higher surface tension (Figure S1, Supporting Information). When the slides were removed, the LM on graphite still maintained the general shapes (Figure S2, Supporting Information). This result also proves the significant reduction of the surface tension of the LM on a graphite substrate. It would provide valuable and promising methods for fabrication of LM planar structures.

The interaction of the LM droplets with the graphite substrate enabled the bouncing smooth LM sphere to be transformed into a dull, flat puddle. When slightly poked with a glass rod, the LM puddle acted like a dull clump of clay. From the observation and discussion above, the interaction between the LM droplets and the graphite substrate have rendered the LM droplet with distinct physical and chemical properties, which are quite different from those on common glass substrate. In order to further illustrate the unique properties thus offered, the LM puddle locomotion and transformation on the graphite surface induced by electrical field were also investigated. The LM and graphite surface were completely immersed in an alkaline electrolyte, which was 0.5×10^{-3} M NaOH in all the experiments in the present study. An external electrical

field was administrated by two steel-wire electrodes connected to a 10 V DC power supply. Through changing the electrode and substrate arrangement, a series of investigations was carried out. The experimental setup and major phenomenon as revealed are summarized in Table 1.

In the first two cases (Case 1 and 2), the transformation of the LM puddle directly connecting with an electric electrode was examined and interpreted (Figure 2a). A previous study has reported some transformation of LM droplets on a common glass substrate with the application of an external electric field.^[13] In this study, through introduction of the graphite, much abundant phenomena were observed where flexible manipulations of the liquid metal can be achieved. An LM puddle with an area of 241.7 mm^2 was placed on graphite immersed in NaOH. The area here and below indicates the 2D image of LM puddle from a bird's-eye view in Figure 2b. The electric field was provided by a 10 V DC power supply with two steel-wire electrodes. When the anode contacted the LM puddle itself (Case 1, Table 1), the LM puddle stretched into a large, thin film with an area of 662.4 mm^2 in 1 s. The LM droplet on the glass substrate had a similar phenomenon when contacted with the anode (Figure S3, Supporting Information). The LM film contracted again into dull puddle by disconnecting the anode from the LM film. In these transformations, the contact with the anode could raise the potential of the LM puddle, which further reduces the surface tension of the LM puddle based on Lippman's equation. When the LM puddle was contacted with the cathode (Case 2, Table 1), the flat LM puddle quickly transformed into a sphere with a smaller area of 48.5 mm^2 . However, the LM droplet on the glass substrate was repulsive to the cathode, which made it even hard to connect the LM with the cathode. Typical snapshots of the same LM puddle transformations in Case 1 and 2 are displayed in Figure 2b. The dynamic processes of Case 1 and Case 2 can be found in Movie S3 and S4 (Supporting Information).

In addition to the transformation, the planar locomotion of the LM puddle on graphite under an electric field was also investigated. The LM droplet was placed on graphite immersed in NaOH and quickly became a dull flat LM puddle. An external electrical field was applied by two steel-wire electrodes connected to a 10 V DC power supply. The electrodes were immersed in NaOH without contacting the graphite or the LM. Therefore, this provided a planar electric field for the LM puddle locomotion. It has been discussed above that the LM puddle was positively charged. Thus, it is not surprising that the puddle slowly moved toward the cathode when the electrical

Table 1. The experimental settings and main phenomenon in the investigation of LM interaction with graphite substrate based on Ga₆₅In₂₂Sn₁₃.

Case	Voltage	Anode	Cathode	Test subject	Main phenomena
1	DC, 10 V	Contact LM; fixed	Not contacted; fixed	Transformation	The flat LM puddle quickly stretched into thinner LM film.
2	DC, 10 V	Not contacted; fixed	Contact LM; fixed	Transformation	The flat LM puddle quickly transformed into a sphere.
3	DC, 10 V	Not contacted; fixed	Not contacted; fixed	Planar locomotion	The flat LM puddle continuously elongated and moves toward the cathode.
4	DC, 10 V	Not contacted; fixed	Not contacted; not fixed	Planar locomotion	The flat puddle of LM elongated, moved toward cathode and could make a turn in any direction with cathode.
5	DC, 10 V	Not contacted; not fixed	Not contacted; fixed	Planar locomotion	The LM puddle moved toward cathode with a notch at the rear end.
6	DC, 10 V	Not contacted; not fixed	Not contacted; not fixed	Upslope locomotion	The slope locomotion of LM puddle was realized.

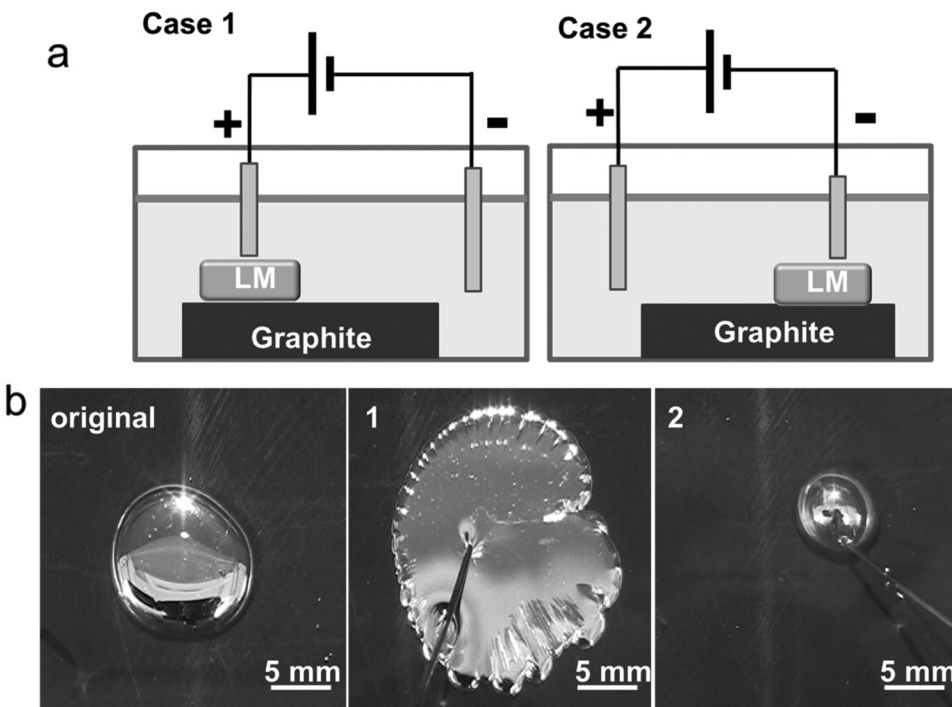


Figure 2. The transformation of LM on graphite induced by direct connection with an electrode. a) Scheme of the experimental Case 1 and Case 2. Case 1: the transformation of the LM on graphite directly connecting an external power anode. Case 2: the transformation of the LM on graphite directly connecting an external power cathode. b) Images of the LM puddle on graphite and its transformations in experimental Case 1 and Case 2.

field was applied in NaOH (Case 3, 4, and 5, Table 1). When both the anode and the cathode were fixed and mounted relatively far away from LM, the LM elongated and moved to the cathode with the rear end being dragged like a tail (Figure 3a). When it moved close to the cathode, the LM puddle branched at the head end, which may be caused by electrochemical reactions (Figure S4, Supporting Information). When the cathode was not fixed and made turns close to the LM puddle (Case 4, Table 1), the head end of the LM puddle made turns along with the cathode movement and the tail was dragged along more slowly (Figure 3b). To further investigate the kinetics of the locomotion mode in Case 3, the directional locomotion of the LM in a particular electric field was examined. The anode and cathode of the external 10 V power supply were separated by 10 cm to provide the desired electric field. When the electricity was switched on, the LM puddle continuously elongated and moved toward the cathode with the rear end being dragged like a tail (Figure 3c), which was quite different from the quick and smooth movement of the LM droplets on a glass surface (Figure S5, Supporting Information). More specifically, it was observed that the thick oxidized surface moved relatively slowly and gradually shrank to the rear end like a tail, while, at the head end, the bright metal with less thick oxidized surface quickly ran to the cathode (Figure S6, Supporting Information). The transient displacement of both the rear and head ends of the two sized LM puddles were recorded and are shown in the inset of Figure 3c. It can be observed that larger sized LM moved faster than the smaller one as a whole. More specifically, when both heads reached the end point (here about 7 cm from the start point), the LM puddle with the larger size also dis-

played a larger deformation, namely the distance between the head and the rear. The LM puddle also moved generally faster under the electric field with higher intensity (Figure S7, Supporting Information). More vivid processes can be found in Movie S5–S7 in the Supporting Information.

The mechanism of morphological transformation and planar locomotion of LM droplets in a common glass Petri dish in NaOH under an electric field has already been discussed in previous reports.^[13] The driving mechanism was similar in our study. To summarize, the deformation and directional locomotion of the LM droplets in an electrolyte were mainly due to the changes in surface tension induced by the potential gradient generated by the electric field. The electric field induced an imbalance of the electron distribution in the LM puddle, which generated a potential gradient from the head to the rear end. At the head end, the voltage drop across the EDL will become lower on the rear end, which results in a higher surface tension and thus a higher pressure on this end, according to Lippman's equation (detailed in Figure S8 in the Supporting Information). As a result, the LM puddle was deformed and propelled toward the cathode of the external power supply. A deformed snapshot of the LM puddle is shown in the inset of Figure 3d and the force analysis is depicted in Figure 3d.

However, there are fundamental differences in LM locomotion between the current findings and previous efforts, in which the substrates were insulated. First, the LM puddle moved toward the cathode rather than the anode because the LM puddle was positively charged due to the oxide layer. Second, the deformation of the LM puddle on graphite was much larger under an electric field. This was because the

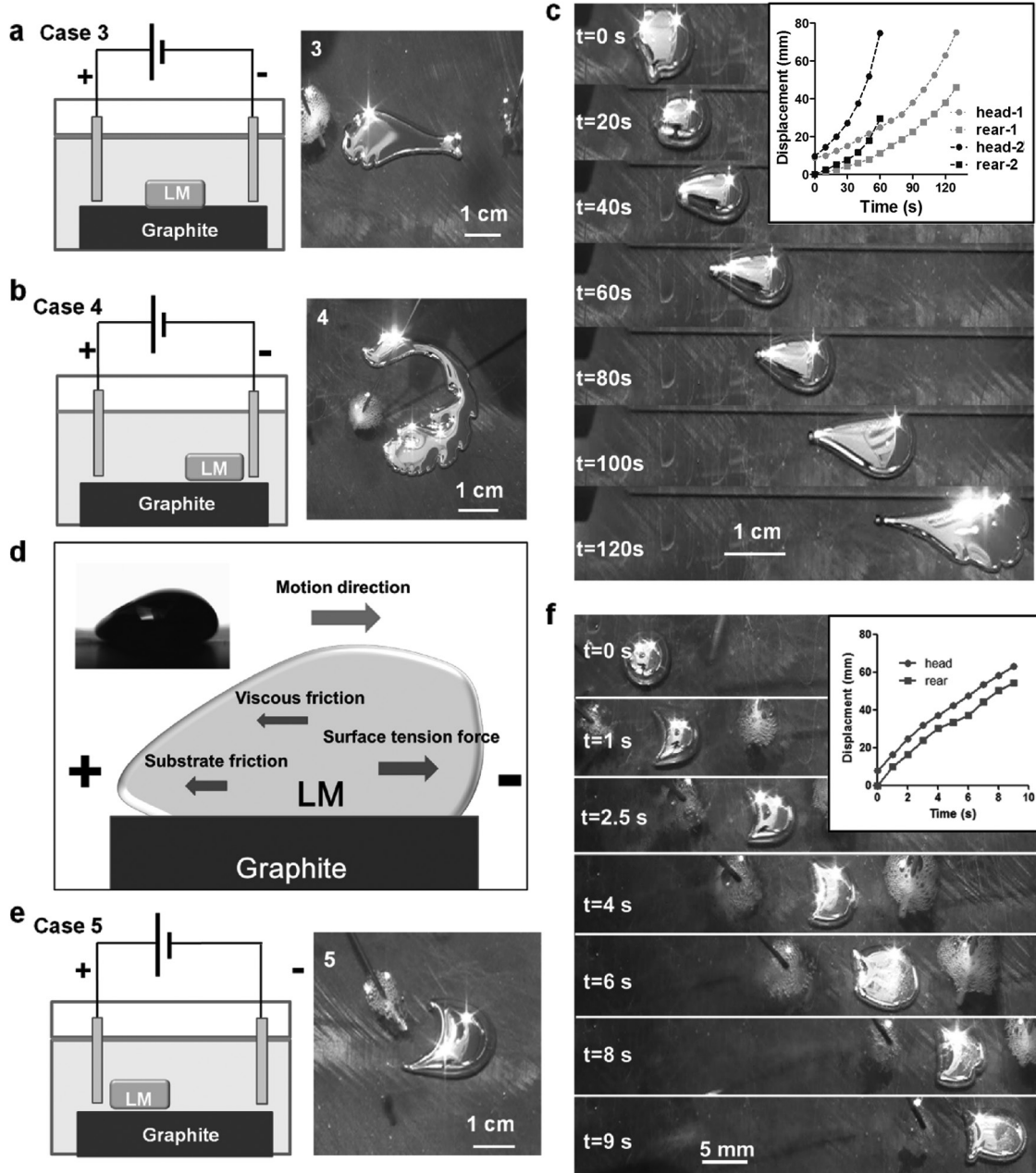


Figure 3. The planar locomotion of the LM on graphite induced by an electric field. a) The scheme of experimental Case 3 and its experimental images. Case 3: the power electrodes were fixed at the opposite sides of LM on graphite. Both electrodes were relatively far away from the LM (over 2 cm). b) The scheme of experimental Case 4 and its experimental images. Case 4: the power cathode was close to the LM on graphite and make turns manually. The anode was fixed relatively far away from the LM. c) Sequential snapshot for an LM directional locomotion in NaOH in Case 3. Inset. The transient displacements of the head and rear ends of the two sized LMs. LM 1: diameter 8.5 mm. LM 2: 9.6 mm. d) The force analysis of the LM on graphite induced by an electric field. Inset. The deformation of the LM puddle on graphite when an electric field was applied. e) The scheme of experimental Case 5 and the experimental image. f) Sequential snapshot for an LM directional locomotion in NaOH in Case 5. Inset. The transient displacements of the head and rear ends of an LM (8.5 mm in diameter).

surface tension of the LM was significantly reduced, which makes the LM more deformable under a certain pressure. Moreover, the oxide layer presented the mechanical properties of a solid, which also influences the locomotion. The thick solid oxide surface could enhance friction with the graphite surface, and thus was left behind at the rear end,

while the LM puddle facing the anode got rid of the thick oxide and moved freely, more like a fluid, although thin oxide layer should still exist over the head part. Therefore, it appears that the bright head end of the LM puddle moved much faster than the rear end with the dark oxide surface (Figure 3c).

In those two directional locomotions in Case 3 and 4, the anodes were placed relatively far away from the LM, say about 2 cm away. When the anode was not fixed and placed close to the rear end of LM at a distance around 0.5 cm, the LM puddle was observed to move more quickly with a meniscus at the rear end (Figure 3e). When the anode and cathode moved together at a distance of \approx 3 cm and the anode was close to the rear end of the LM puddle at a distance around 0.5 cm, the LM puddle was observed to move more quickly than that in Case 3 (Figure 3a). The dynamic process is displayed in Movie S8 in the Supporting Information. The quantified transient locomotion displacement of an LM puddle also proved this (Figure 3 inset; Movie S9, Supporting Information). In such a case, apart from providing the electric field to induce the charge imbalance along the LM, the anode also played another important role in the locomotion of the LM. Here, at the rear end, the LM was electrochemically reduced and the surface tension increased, which pulled the LM backward to form a reverse meniscus, as explained in Figure S9 in the Supporting Information. Thus, the anode worked like a propeller and the LM moved faster than that in Case 3.

Based on the above observations and discussions, the LM puddle presents some unique properties in planar locomotion due to the large surface friction between the LM puddle and the graphite substrate. Besides, when the LM puddle moved under the electric field with the “anode propeller” (Case 5), it wriggled like a worm. Although they have no feet, such worms display amazing ability, say moving even on a sharp slope via a wriggling style. Inspired by this, the slope locomotion of the LM puddle was also examined (Case 6, Table 1).

According to our experiments and also common sense, the sharper the slope is, the more difficult it would be for the LM to climb under the same electric field. In the present experiments for slope locomotion, a 10° graphite slope with a length of 7 cm was prepared. It was neither too flat nor too sharp, which is better for us to present the generalized locomotion properties of LM puddle on graphite slope. In this case, the LM droplet was gently placed on a graphite slope. The cathode was placed on the upward side, close to the head end of the LM puddle and the anode was placed on the downward side at the rear end as indicated in Figure 4a. The distance between the two power electrodes was around 2.5 cm. The voltage was

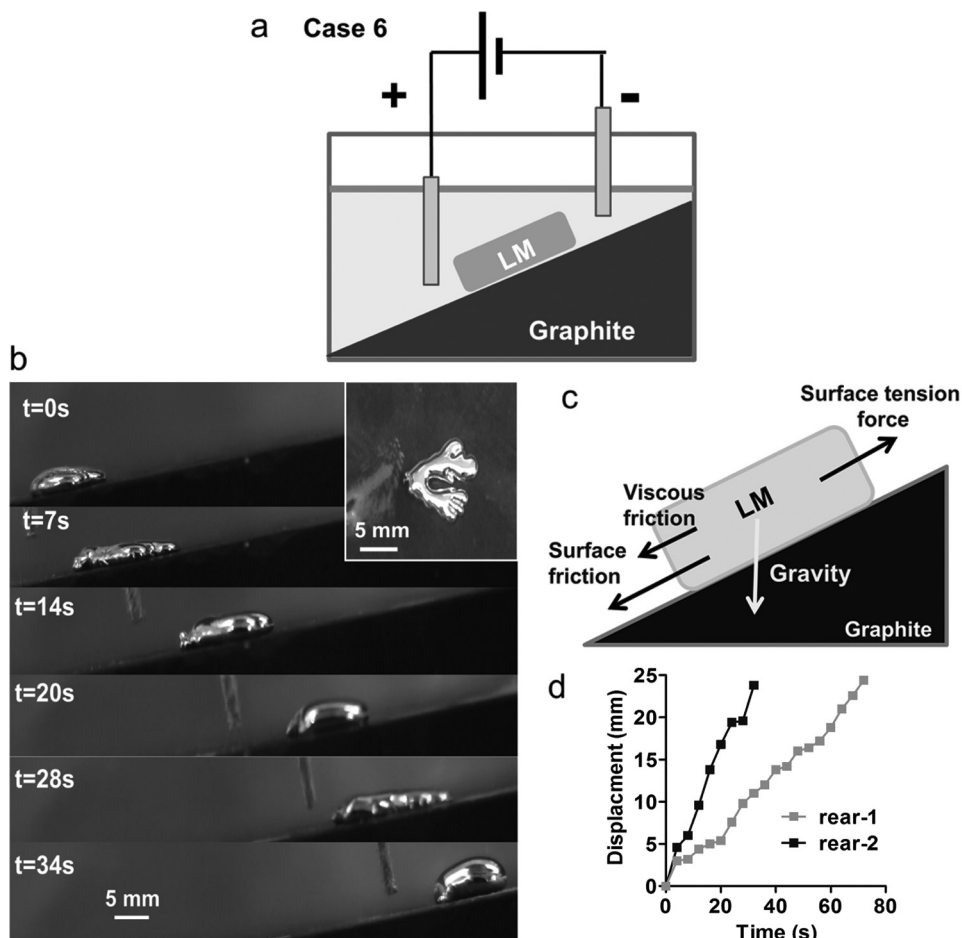


Figure 4. The upslope locomotion of the LM on graphite under an electric field. a) The scheme of experimental setup in slope locomotion. b) Sequential snapshot for LM slope locomotion on graphite in NaOH from the front view. Inset: The plan-view image of a branching LM puddle (8 mm in diameter) during slope locomotion. c) The force analysis of the LM on a graphite slope during locomotion. d) The transient locomotion of two sized LM puddles on graphite slope. The displacement of the rear ends was recorded. The rear 1 (gray squares) indicates the smaller LM puddle with a diameter of 6.7 mm. The rear 2 (black squares) indicates the larger one with a diameter of 8 mm on graphite.

set at 10 V. A gap at about 2–3 mm had to be kept between the bottom of the electrodes and the graphite surface to avoid notable charging of graphite, as well as the LM puddle on it. When no electric field was applied, the LM puddle slid down due to its own gravity. When the electricity was switched on, the LM puddle slowly wriggled up the slope. The head end was continuously branching and the rear end was propelled by the “anode propeller”. Front-view snapshots of the slope climbing of the LM puddle are shown in Figure 4b and a plan-view of the branching LM on the slope is displayed in the inset of Figure 4b. More plan-view snapshots of the slope-climbing process of the LM are shown in Figure S10 in the Supporting Information. The dynamic process of the upslope locomotion is displayed in Movie S10 in the Supporting Information. As the head end was branching, the LM puddle may be divided into separated parts along the upslope locomotion. Thus, the anode and cathode had to coordinate with the locomotion of the LM to avoid dividing. In the example shown in Figure 4b, the cathode was at a distance of around 1–1.5 cm ahead of the head end of the LM puddle and the anode was around 0.5 cm behind the rear end. If the cathode was too far away from the head end, the LM puddle would not move upward due to the insufficient driving force. If it is too close, the head end kept branching and could not move on. In addition, if the anode was too close to the rear end of LM puddle, the repulsive force from the anode could lift up the rear end, making it detached. The detached LM puddle would then become a sphere at once and quickly roll down the slope. Unlike the planar locomotion, the upslope locomotion of LM was significantly affected by the component of gravity (Figure 4c). Subjected to those forces, the LM with the lower surface tension crept upslope like a worm, which was intriguing and unique.

Subsequently, the general kinetic properties of the LM puddle's upslope locomotion on graphite were examined. The transient displacements of two sized LM puddles (6.7 and 8 mm, respectively) on a graphite slope are shown in Figure 4d. The distance between the two electrodes was around 2.5 cm and the LM puddles were not divided separately along the upslope locomotion. Obviously, the larger LM puddle moved more quickly than the smaller one. When the LM puddle was too small (diameter less than about 3 mm), it may be quickly electrochemically oxidized. Thus, it was somewhat difficult to induce obvious locomotion.

Similar to the controllable planar locomotion of the LM droplets, the upslope locomotion of the LM puddle on the graphite substrate could be also regulated by changing the electrical-field intensity. Thus, regulated upslope locomotion can be programmable. In principle, the speed and slope angle of this upslope locomotion can be controlled by regulating the electric-field intensity and electrode position. However, the arrangement of the electric field and electrode position was more complex. In the upslope locomotion, the distance between the electrodes and the LM puddle had to be carefully controlled to avoid the LM dividing or detaching from the graphite. When the electric-field intensity increased, the electrochemically induced branching at the head end became more remarkable, which requires the careful manipulation of the anode to coalesce and propel the branched LM puddle in order to realize the upslope locomotion. Moreover, the increase of the electric-field intensity may induce electrochemical reactions on the LM, which could affect the surface charge distribution as well as the surface

tension. As a result, the stressed condition of LM puddle would also change.

In summary, a group of fundamental phenomena in the manipulation of LM electrochemically enabled by graphite have been revealed. The induced transformation uniformly reduced the surface tension of the LM in the electrolyte without an external energy supply, which is valuable in applications such as LM-based structure patterning. Based on this discovery, an electric-field-induced planar transformation of the LM on the graphite surface was also clarified. Moreover, the unique planar and upslope locomotion of the LM on graphite was first observed with the application of a low-voltage DC electric field, which may provide new insight for potential soft device manufacture. Furthermore, the electrochemical properties of the LM as raised in this study also suggest further explorations worth pursuing in the near future. Above all, the intriguing and inspiring findings presented in the current paper may provide further opportunities for advancing liquid-metal science.

Experimental Section

Materials and Methods: The experiments were carried out on the eutectic liquid-metal GaInSn alloy (65%, In 22%, Sn 13% by mass) immersed in a 0.5×10^{-3} M NaOH solution. The GaInSn alloy was prepared from gallium, indium, and tin with purity of 99.99%. These raw materials with mass ratios of 67:12:12.5 were added into a beaker and were heated to 100 °C. A magnetic stirrer was used to stir the mixture uniformly after the metals had all melted. Subsequently a series of experiments, as listed in Table 1 were carried out. The graphite plate with purity of 99.9% was 10 cm × 10 cm × 1 cm in length, width, and height. In the experimental Cases 1–4, the graphite plates were placed horizontally. In Case 5, the graphite slope was prepared by elevating one side of the graphite plate with small graphite pads. The angles of the slope could be regulated by changing the positions of the graphite pads. Digital video equipment Sony HDR-PJ670 and macro SLR camera Canon EOS 70D were used to record the experimental phenomenon.

Raman Measurement: A Raman microscope (inVia-Reflex, Renishaw) was used to determine the composition of surface oxide with a 532 nm laser as the excitation source. A 10x objective lens is used to focus the excitation laser and to collect Raman spectra in back reflection.

Zeta-Potential Measurement: Alkaline solutions with different pHs were prepared with NaOH and diluted water. The nanoparticles were purchased from DK Nano Technology Co. Beijing. The concentration of each conductive nanoparticle was: 0.15 mg mL⁻¹ graphite, 0.3 mg mL⁻¹ copper, and 0.4 mg mL⁻¹ steel, respectively. Then the zeta potential of those nanoparticles were measured by the Beckman Coulter DelsaNano C Zeta Potential Analyzer (USA).

Supporting Information

Supporting Information is available from the Wiley Online Library or from the author.

Acknowledgements

This work was currently supported by the Dean's Research Funding of the Chinese Academy of Sciences and Beijing Municipal Science and Technology Funding (Under Grant No. Z151100003715002).

Received: March 25, 2016

Revised: July 21, 2016

Published online:

- [1] a) Y. Zheng, Z. He, Y. Gao, J. Liu, *Sci. Rep.* **2013**, *3*, 1786; b) M. Kubo, X. Li, C. Kim, M. Hashimoto, B. J. Wiley, D. Harn, G. M. Whitesides, *Adv. Mater.* **2010**, *22*, 2749; c) J. W. Boley, E. L. White, G. T. C. Chiu, R. K. Kramer, *Adv. Funct. Mater.* **2014**, *24*, 3501.
- [2] a) M. G. Pollack, R. B. Fair, A. D. Shenderov, *Appl. Phys. Lett.* **2000**, *77*, 1725; b) J.-H. So, M. D. Dickey, *Lab Chip* **2011**, *11*, 905.
- [3] S.-Y. Tang, K. Khoshmanesh, V. Sivan, P. Petersen, A. P. O'Mullane, D. Abbott, A. Mitchell, K. Kalantar-Zadeh, *Proc. Natl. Acad. Sci. USA* **2014**, *111*, 3304.
- [4] J. Zhang, Y. Yao, L. Sheng, J. Liu, *Adv. Mater.* **2015**, *27*, 2648.
- [5] a) A. Elliott, T. Pollock, S. Tin, W. King, S.-C. Huang, M. Gigliotti, *Metall. Mater. Trans. A* **2004**, *35*, 3221; b) J. Y. Zhu, S.-Y. Tang, K. Khoshmanesh, K. Ghorbani, *ACS Appl. Mater. Interfaces* **2016**, *8*, 2173; c) K. Ma, J. Liu, *Front. Energy Power Eng. Chin.* **2007**, *1*, 384.
- [6] N. Morley, J. Burris, L. Cadwallader, M. Nornberg, *Rev. Sci. Instrum.* **2008**, *79*, 056107.
- [7] M. Gao, L. Gui, *Lab Chip* **2014**, *14*, 1866.
- [8] H.-J. Kim, T. Maleki, P. Wei, B. Ziaie, *J. Microelectromech. Syst.* **2009**, *18*, 138.
- [9] a) S. Cheng, Z. Wu, *Lab Chip* **2010**, *10*, 3227; b) S. H. Jeong, A. Hagman, K. Hjort, M. Jobs, J. Sundqvist, Z. Wu, *Lab Chip* **2012**, *12*, 4657.
- [10] Q. Wang, Y. Yu, J. Yang, J. Liu, *Adv. Mater.* **2015**, *27*, 7109.
- [11] a) S. Y. Tang, V. Sivan, P. Petersen, W. Zhang, P. D. Morrison, K. Kalantarzadeh, A. Mitchell, K. Khoshmanesh, *Adv. Funct. Mater.* **2014**, *24*, 5851; b) A. F. Chrimes, K. J. Berean, A. Mitchell, G. Rosengarten, K. Kalantar-Zadeh, *ACS Appl. Mater. Interfaces* **2016**, *8*, 3833.
- [12] S.-Y. Tang, V. Sivan, K. Khoshmanesh, A. P. O'Mullane, X. Tang, B. Gol, N. Eshtiaghi, F. Lieder, P. Petersen, A. Mitchell, *Nanoscale* **2013**, *5*, 5949.
- [13] L. Sheng, J. Zhang, J. Liu, *Adv. Mater.* **2014**, *26*, 6036.
- [14] a) D. Rus, M. T. Tolley, *Nature* **2015**, *521*, 467; b) C. Majidi, *Soft Robotics* **2014**, *1*, 5; b) S. Kim, C. Laschi, B. Trimmer, *Trends Biotechnol.* **2013**, *31*, 287; c) R. F. Shepherd, F. Ilievski, W. Choi, S. A. Morin, A. A. Stokes, A. D. Mazzeo, X. Chen, M. Wang, G. M. Whitesides, *Proc. Natl. Acad. Sci. USA* **2011**, *108*, 20400.
- [15] J. Zhang, L. Sheng, J. Liu, *Sci. Rep.* **2014**, *4*.
- [16] R. Rao, A. M. Rao, B. Xu, J. Dong, S. Sharma, M. Sunkara, *J. Appl. Phys.* **2005**, *98*, 94312.